Physical Characterization of the Hydrates of Urapidil

S. A. BOTHA*[x], M. R. CAIRA[‡], J. K. GUILLORY[§], AND A. P. LÖTTER*

Received May 18, 1987, from the *Research Institute for Industrial Pharmacy, University of Potchefstroom for C.H.E., Potchefstroom 2520, South Africa, the ‡Crystallography Group, Department of Physical Chemistry, University of Port Elizabeth, Port Elizabeth 6000, South Africa, and the §College of Pharmacy, University of Iowa, Iowa City, IA 52242. Accepted for publication November 18, 1987.

Abstract □ Three hydrates of urapidil were prepared and characterized by means of differential scanning calorimetry, thermogravimetric analysis, infrared spectroscopy, X-ray powder diffraction, intrinsic dissolution rates, and solution calorimetry. The stoichiometry of the urapidil hydrates was found to be 1:5, 1:3, and 1:1 (urapidil:water). The crystal and molecular structures of urapidil pentahydrate were determined from three-dimensional X-ray data. The stability of the pentahydrate and monohydrate under different storage conditions was also determined.

Urapidil, 6-[[3-[4-(*o*-methoxyphenyl)-1-piperazinyl]propyl]amino]-1,3-dimethyluracil, is a new antihypertensive drug, the efficacy of which has been demonstrated in animals,[1] as well as in humans.[2] In previous publications, the physicochemical properties of three nonsolvated forms of urapidil,[3] as well as a methanol solvate,[4] were reported.

This paper deals with the physicochemical properties and X-ray studies of three hydrated forms of urapidil. These hydrates were characterized from their thermal behavior, thermogravimetric analysis, X-ray diffraction, IR spectra, intrinsic dissolution rates, solution calorimetry, and scanning electron microscopy.

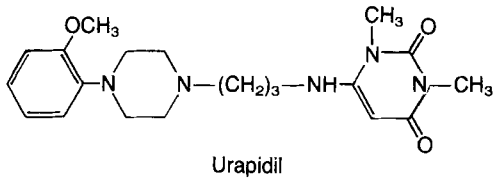

Urapidil

Experimental Section

Preparation of Urapidil Hydrates—Commercial urapidil (Byk-Gulden) was used in the preparation of the hydrates. Purity determinations were performed using differential scanning calorimetry (DSC), and purity of 99.73 ± 0.06% was found. Urapidil does not form a solvate when recrystallized from 100% ethanol, 95% ethanol, or denatured ethanol. However, when recrystallized from water:ethanol (1:1; 16% m/v solute) or from water:ethanol (3:1; 4% m/v solute), two different hydrates, a pentahydrate and a trihydrate, respectively, are formed. A monohydrate was obtained by the recrystallization of a saturated solution of urapidil from boiling water.

Thermal Analysis—The thermograms of the hydrates were recorded on a Perkin-Elmer differential scanning calorimeter (DSC-2) equipped with a model 3600 data station, calibrated with pure indium (99.999%, mp 156.60 °C), and this calibration was checked using a lead standard (purity 99.999%, mp 327.27 °C). The samples were measured into aluminum pans and the lids were crimped onto the pans with the aid of a Du Pont model 70033 crimper. An empty pan, sealed in the same way as the sample, was used as reference. The thermal behavior of the three hydrates of urapidil was studied under a nitrogen purge at a heating rate of 10 °C min^{-1}.

Thermal gravimetric analyses (TGA) were performed using the Perkin-Elmer TGS-2 thermogravimetric system and the thermal analysis model 3600 data station. The temperature axis was calibrated using the ferromagnetic materials furnished by Perkin-Elmer. Analyses were performed on samples in platinum pans at a heating rate of 10 °C min^{-1} under nitrogen purge.

X-ray Powder Diffraction—Powder diffractograms were recorded on an automated Philips PW1050/70 diffractometer using FeKα radiation (λ = 1.937 Å). The pentahydrate was finely ground, screened through 75-μm mesh, and packed in a standard Al sample holder. The powder pattern was recorded under the following conditions: 40 kv, 30 mA, range 10^4 cps, time constant 4, scan rate 1° 2θ min^{-1}, angular range 10–45° 2θ, divergence slit 1°, scatter slit 0.2°, receiving slit 1°.

Diffractograms for the trihydrate and monohydrate of urapidil were also recorded. However, due to their relative instability and texture, difficulties were encountered in obtaining uniformly ground samples, and the recording conditions described above could not be duplicated. The trihydrate was ground to a fine slurry under an ethanol:water (1:3) solution, the surface layer was allowed to dry, and the pattern was recorded at an increased scan rate of 2° 2θ min^{-1} over a smaller angular range (10–35° 2θ), which included the major peaks. Paucity of fresh monohydrate sample prevented the use of the standard Al holder, and the pattern was recorded from a thin layer of ground material spread on a glass plate. A sample of the pentahydrate was heated at 120 °C under reduced pressure for 20 min to obtain the desolvated material whose diffractogram was recorded under the same conditions as described for the monohydrate.

Single Crystal X-ray Analysis—Crystals of urapidil pentahydrate were found to be monoclinic, space group $P2_1/n$ (from systematic absences h01 h + 1 = 2n + 1, 0k0 k = 2n + 1). Intensity data were collected from a prismatic specimen (0.275 × 0.350 × 0.375 mm) mounted on a Philips PW1100 four-circle diffractometer. Accurate cell parameters were determined by least-squares analysis of angular data for 25 high-order reflections. A total of 3714 intensities were measured by the ω-2θ scan technique (scan width 1.3° θ, speed 0.052° θ s^{-1}) with graphite-monochromated MoKα radiation (λ = 0.7107 Å), the background being measured on each side of the peak for half the peak scan time. Three reference reflections were monitored every hour; their intensities deviated randomly by only ±3% from the mean, indicating crystal stability.

After data reduction and correction for Lorentz polarization effects, 2200 reflections with $F_o > 3\sigma(F_o)$ were retained and used in the final analysis. The structure was solved by the direct method using the SHELX76 program.[5] Initially, only the urapidil molecule was sought, and it was located in an E-map phased with 485 reflections with E > 1.30. Five further unique peaks were located from successive difference Fourier maps and were assigned as oxygen atoms of water of crystallization on the basis of their electron densities and geometrical considerations. Suitable candidates as H atoms of the H_2O molecules were found at an advanced stage of the refinement.

The final model included the following features: all non-H atoms thermally anisotropic [except N(1) and C(6) which displayed isotropic behavior and were treated as such owing to core-storage limitations], all H atoms isotropic; N—H and O(W)—H bond lengths constrained to 1.00 (±0.05–0.10) Å, all other H atoms geometrically fixed at C—H = 1.08 Å in a riding model; and U_{iso} for solvate H atoms fixed at those of parent O(W) atoms, U_{iso} for other H atoms refined as free variables for four chemically different groups. After the final cycle of full-matrix least-squares refinement, in which $\Sigma w(F_o - F_c)^2$ was minimized ($w = 1/\sigma^2(F_o)$), the range for O(W)—H was 0.77(5)–0.97(6) Å, and that for H—O(W)—H was 106(4)–118(6)°. The average Δ/σ was $<10^{-3}$, with a maximum of 0.01, and the final agreement factors were R = 0.074, Rw = 0.061, and S = 1.769 for 334 parameters. Background fluctuations in a final difference map ranged from −0.37 to 0.44 e $Å^{-3}$

0022-3549/88/0500-0444$01.00/0

Figures were drawn with the CRISTEP[6] program, and molecular parameters were calculated with the PARST[7] program. Full lists of derived geometrical parameters and observed and calculated structure factors are available on request.

Infrared Spectra—Nujol mulls of the powdered crystals were prepared and the spectra determined over a wave-number range of 4600 to 800 cm^{-1} using a Nicolet FDX Fourier transform infrared spectrophotometer that was connected to a Nicolet 5DX data processor.

Intrinsic Dissolution Rates—The intrinsic dissolution rates of the hydrates were determined by use of a propeller-driven stirrer apparatus.[3,8] Prior to mounting the compressed disk in the holder for the dissolution study, a scraping was obtained from the protected side of the pellet. The DSC thermograms at both 10 and 1 °C min^{-1} were obtained from this scraping in order to determine what changes occurred in the sample during the compression process. At the conclusion of the dissolution experiment, the surface of the pellet exposed to the dissolution medium was sampled and DSC thermograms were obtained to determine what changes took place in the tablet during the dissolution run.

Solution Calorimetry—The heats of solution of the hydrates were determined by solution calorimetry, using the method described in an earlier publication.[3]

Scanning Electron Photomicrographs—Photomicrographs were obtained using the Cambridge Stereoscan 250 scanning electron microscope. Since the crystals had to be completely dry before the samples could be prepared for photomicrographs, the different solid samples of the hydrates were stored under reduced pressure for 3 d, after which the samples were coated under reduced pressure with carbon (Emscope TB 500 Sputter Coater) before being coated with a thin gold platinum film (Eiko Engineering Ion Coater IB-2).

Stability of the Hydrates—Samples (50 mg) of the penta- and monohydrates were stored in amber, loosely stoppered containers. The samples were stored under the following conditions: for three months at room temperature, 37 °C, and 37 °C and 80% relative humidity, after which time DSC and TGA thermograms were obtained. Samples were also stored at 45 °C for one and three months, respectively, and DSC and TGA thermograms were obtained.

Results and Discussion

The crystals obtained by crystallization from water:ethanol (1:1; pentahydrate), water:ethanol (3:1; trihydrate), and water (monohydrate) were identified using data from TGA, thermal analysis, X-ray powder diffraction, IR, intrinsic dissolution rates, solution calorimetry determinations, and scanning electron microscopy. Complete structural elucidation of the pentahydrate was effected by single-crystal X-ray methods.

Differential Scanning Calorimetry and Thermogravimetric Analysis Profiles—*Urapidil Pentahydrate*—Based on the DSC thermograms, these crystals typically show a broad endotherm ranging from ~45 to 90 °C. The endothermic peak corresponding to solvent loss usually exhibits a maximum near 70 °C and shoulders near 65 and 90 °C (Figure 1). The position of the latter peak varies considerably from one sample to the next, as does its area.

Since the boiling point of ethanol is 78.5 °C, it was difficult, based on TGA and DSC thermograms, to reach a definite conclusion whether this is urapidil:water or a urapidil:water:ethanol solvate. A Karl Fischer water titration was performed on a freshly recrystallized sample and the total amount of moisture content of the crystals was found to be 18.4%. This result correlated extremely well with the TGA thermogram, which had indicated a total loss of 19.0% of moisture.

The loss of water occurred over two stages, leading one to conclude that this crystal form is a hydrate of the form urapidil:water (1:2) with adsorbed water. However, the single-crystal X-ray crystallographic data obtained confirmed that this crystal form is a pentahydrate. The two distinct stages of mass loss were assumed to be due to two different types of binding sites for water in the crystal lattice. Urapidil

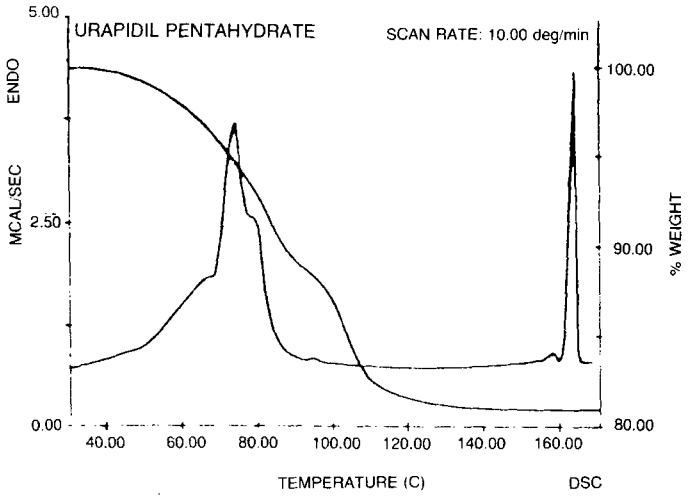

Figure 1—*The DSC and TGA thermograms of urapidil pentahydrate.*

pentahydrate should theoretically contain 18.85% of water, but the moisture content varied considerably from one sample to the next. The highest moisture content found was 22.1% water, with a mean value of 17% for seven different determinations. When all solvent was removed from the pentahydrate by drying over phosphorus pentoxide, the "desolvate" consisted primarily of urapidil Form I.[3]

Urapidil Trihydrate—Based on the DSC thermograms, these crystals typically show a broad endotherm ranging from ~45 to 75 °C. This endothermic peak, corresponding to solvent loss, exhibits a maximum near 70 °C (Figure 2).

A hydrate of the form urapidil:water (1:3) should contain 12.33% of water. The TGA showed a mean mass loss of 11.2%, with some of the loss apparently due to surface adsorbed water.

A urapidil trihydrate sample containing a total amount of 12.9% of water was stored in a desiccator over water. Following 3 d of exposure to high humidity, the crystals showed a total mass loss on heating amounting to 13.4%. It was concluded that the trihydrate did not change to a higher hydrate on exposure to high humidity; the increase in water loss was due to an increase in surface adsorbed water.

Urapidil Monohydrate—The DSC thermograms of the monohydrate show a broad endotherm ranging from 45 to 90 °C. This endothermic peak, corresponding to solvent loss, exhibits two maxima, one near 65 °C and the other near 80 °C (Figure 3).

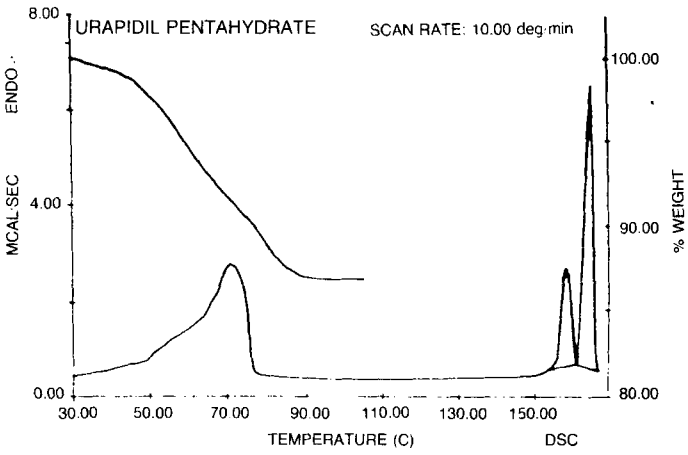

Figure 2—*The DSC and TGA thermograms of urapidil trihydrate.*

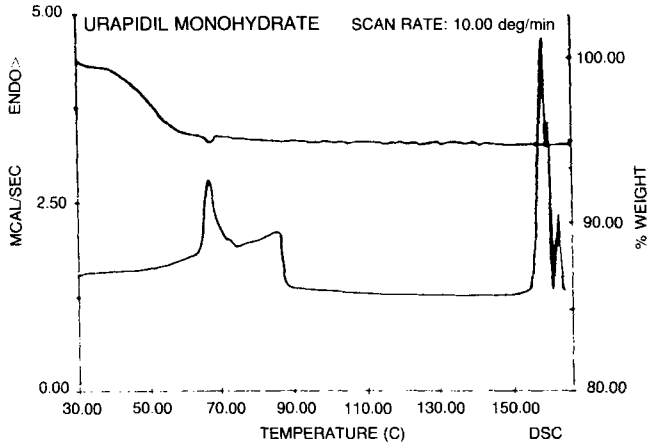

Figure 3—*The DSC and TGA thermograms of urapidil monohydrate.*

A hydrate of the form urapidil:water (1:1) should contain 4.44% of water. Thus, based on TGA analysis (Figure 3), it is concluded that, on recrystallization from water, a monohydrate is formed. When this lower hydrate was stored for 2 d in a desiccator over water, it was converted to a pentahydrate.

Infrared Spectroscopy—Only slight differences could be detected between the three anhydrous forms of urapidil.[3] However, the IR spectrum of the pentahydrate is substantially different from those of the anhydrous forms. A comparison of the IR spectra of the anhydrous Form II of urapidil, the methanol solvate, and the pentahydrate can be seen in Figure 4. The main differences between urapidil Form II and the pentahydrate in the 950–1700-cm^{-1} range are indicated by arrows (Figure 4).

The O—H absorption band, due to water, can be found at 3279 to 3479 cm^{-1}, with a maximum at 3451.6 cm^{-1}, while the secondary amine absorption band of urapidil can be found at 3099 to 3279 cm^{-1}, with a maximum at 3223.5 cm^{-1}.

X-ray Powder Diffraction—Figure 5 shows the powder pattern of urapidil pentahydrate; the *d*-spacings for the six most intense peaks are included. Despite differences in recording conditions necessitated by the nature of the samples, the powder patterns of the three hydrated species were compared and showed very similar features. Close correlation between peak positions was observed for the pentahydrate and the trihydrate. Major peaks in the powder pattern of the monohydrate had counterparts in that of the trihydrate. The powder pattern of the desolvated sample (Form I)[3] was, however, markedly different from those of the hydrates. In the absence of single-crystal diffraction data for all of the hydrates, it is thus tentatively suggested that their crystal structures are essentially the same, differing primarily in the spatial distribution of water molecules of crystallization. This interpretation is consistent with the finding, from three dimensional X-ray data, that in the pentahydrate crystal, water molecules are localized in channels.

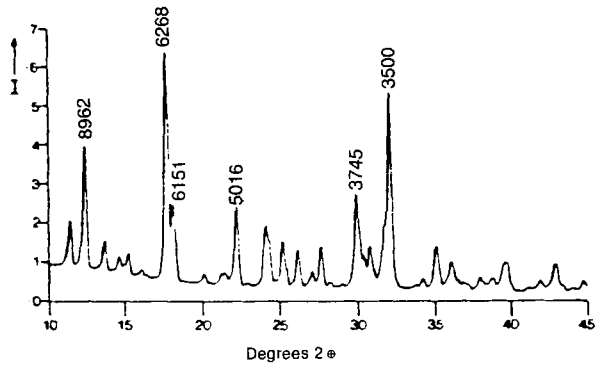

Figure 5—*The X-ray powder pattern of urapidil pentahydrate (on the intensity scale of 1.0 ≡ 10^4 cps).*

Intrinsic Dissolution Rates—For a dissolving disk with an essentially constant surface area, the dissolution process can be described by

$$W = kC_s t \quad (1)$$

where W is the amount dissolved, C_s is the solubility of the substance at time t, and the constant k includes the surface area of the dissolving disk, the diffusion coefficient, and the diffusion layer thickness.[9] Thus, a plot of amount dissolved as a function of time should be linear for the initial dissolution stages, and intrinsic dissolution rates (kC_s/surface area of the dissolving disk) can be calculated from the slopes of the straight lines.

On compression of the different hydrates into disks, no change could be observed in the DSC thermograms. In addition, no change was observed after the dissolution rate determinations. The dissolution rate plots of the pentahydrate, trihydrate, and monohydrate of urapidil in water at 37 °C were linear (Figure 6), with no initial curvatures or faster initial dissolution rates.

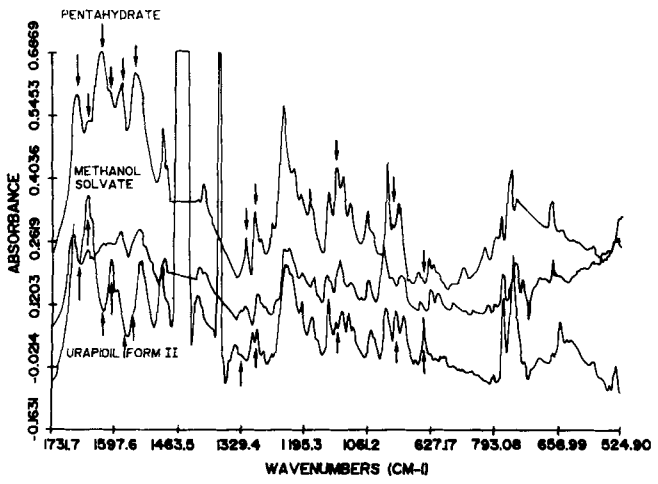

Figure 4—*The IR spectrum of urapidil pentahydrate.*

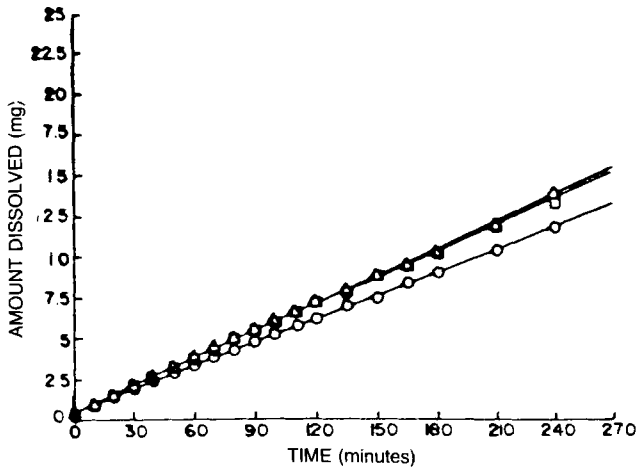

Figure 6—*Dissolution rate plots of the pentahydrate (○), trihydrate (□), and monohydrate (△) in water at 37 °C.*

The intrinsic dissolution rates of the three hydrates, as well as a comparison with the intrinsic dissolution rates of the three anhydrous forms and the methanol solvate of urapidil, are given in Table I.

Solution Calorimetry—*Pentahydrate*—In order to eliminate mass bias in the data, six samples of the pentahydrate, ranging in mass from 30 to 75 mg, were used to determine the heat effect. A plot of heat of solution versus sample mass was constructed (Figure 7), and the heat effect of known quantities was determined from the slope of the plot of the form

$$y = 3.463 \times 10^{-2}x - 0.003 \quad (2)$$

with a correlation coefficient of 0.99996.

The heat absorbed on dissolution in 95% ethanol at 30 °C, as calculated from the slope of the equation and correcting for the effect of ampule breaking and other instrumental factors, was 69.16 kJ mol^{-1} (16.54 kcal mol^{-1}). When the heat absorbed was calculated for the different quantities, the mean heat effect was 69.08 ± 0.20 kJ mol^{-1}, with no correction for instrumental factors.

Trihydrate—The heat effect was determined from the slope of the plot of the form

$$y = 2.880 \times 10^{-2}x + 0.003 \quad (3)$$

with a correlation coefficient of 0.99903 (Figure 7).

The heat absorbed on dissolution, as calculated from the slope of the above equation, was 53.20 kJ mol^{-1} (12.72 kcal mol^{-1}). When calculated for different quantities, the mean heat effect was 53.50 ± 0.81 kJ mol^{-1} (12.74 ± 0.19 kcal mol^{-1}).

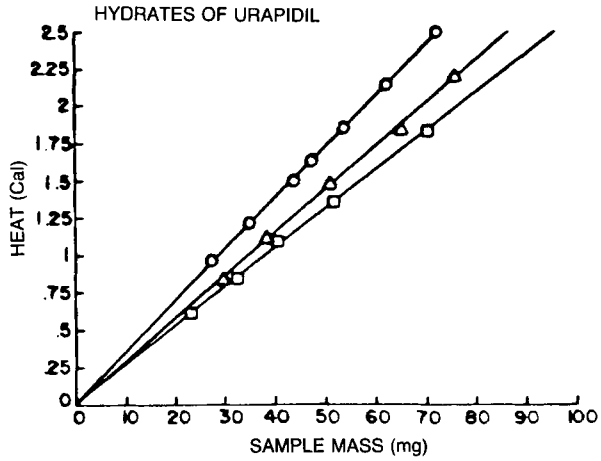

Figure 7—*Solution calorimetry determinations on the pentahydrate* (○), *trihydrate* (△), *and monohydrate* (□).

Table I—Intrinsic Dissolution Rates of the Hydrates of Urapidil in Water at 37 °C

Crystalline Form	Initial Dissolution Rate, mg L^{-1} cm^{-2} min^{-1}	Final Dissolution Rate, mg L^{-1} cm^{-2} min^{-1}
Hydrates		
Pentahydrate	—	0.95×10^{-4}
Trihydrate	—	0.99×10^{-4}
Monohydrate	—	1.03×10^{-4}
Methanol solvate obtained from:		
Methanol:water (1:1)	3.65×10^{-4}	0.56×10^{-4}
2% Solution in methanol	3.87×10^{-4}	0.62×10^{-4}
3% Solution in methanol	Curvature	0.80×10^{-4}
Anhydrous Forms		
I	—	0.68×10^{-4}
II	4.16×10^{-4}	0.68×10^{-4}
III[a]	3.34×10^{-4}	—

[a] Mainly Form III.

Table II—Comparison of the Heat of Solution for the Anhydrous Forms, the Methanol Solvate, and the Hydrates of Urapidil

Crystalline Forms of Urapidil	Heat of Solution, kJ mol^{-1}
Form I	21.96
Form II	24.26
Form III	22.98 (estimated)
Methanol solvate	48.39
Pentahydrate	69.16
Trihydrate	53.50
Monohydrate	44.28

Table III—Behavior of Urapidil Pentahydrate under Various Conditions: Thermogravimetric Analysis Studies

Storage Time, months	Conditions of Storage	Temperature Range, °C	Mass Loss, % m/m	Temperature Range, °C	Mass Loss, % m/m
0	—	30.5–102.8	16.21	102.8–134.6	2.49
3	room temp	30.1– 86.4	12.55	86.4–135.6	5.24
3	37 °C	30.1–159.1	0.01	—	—
3	37 °C; 80% RH	30.0– 92.6	15.19	92.6–135.6	3.43
1	45 °C	30.2–134.7	0.43	—	—
3	45 °C	30.1–155.2	0.00	—	—

Table IV—Behavior of Urapidil Monohydrate under Various Conditions: Thermogravimetric Analysis Studies

Storage Time, months	Conditions of Storage	Temperature Range, °C	% Water Loss, m/m
0	—	32.4–115.9	4.71
3	room temp	33.4– 92.5	2.48
3	37 °C	30.1–150.6	0.08
3	37 °C; 80% RH	30.1–108.4	15.30
3	45 °C	30.1–124.8	0.04

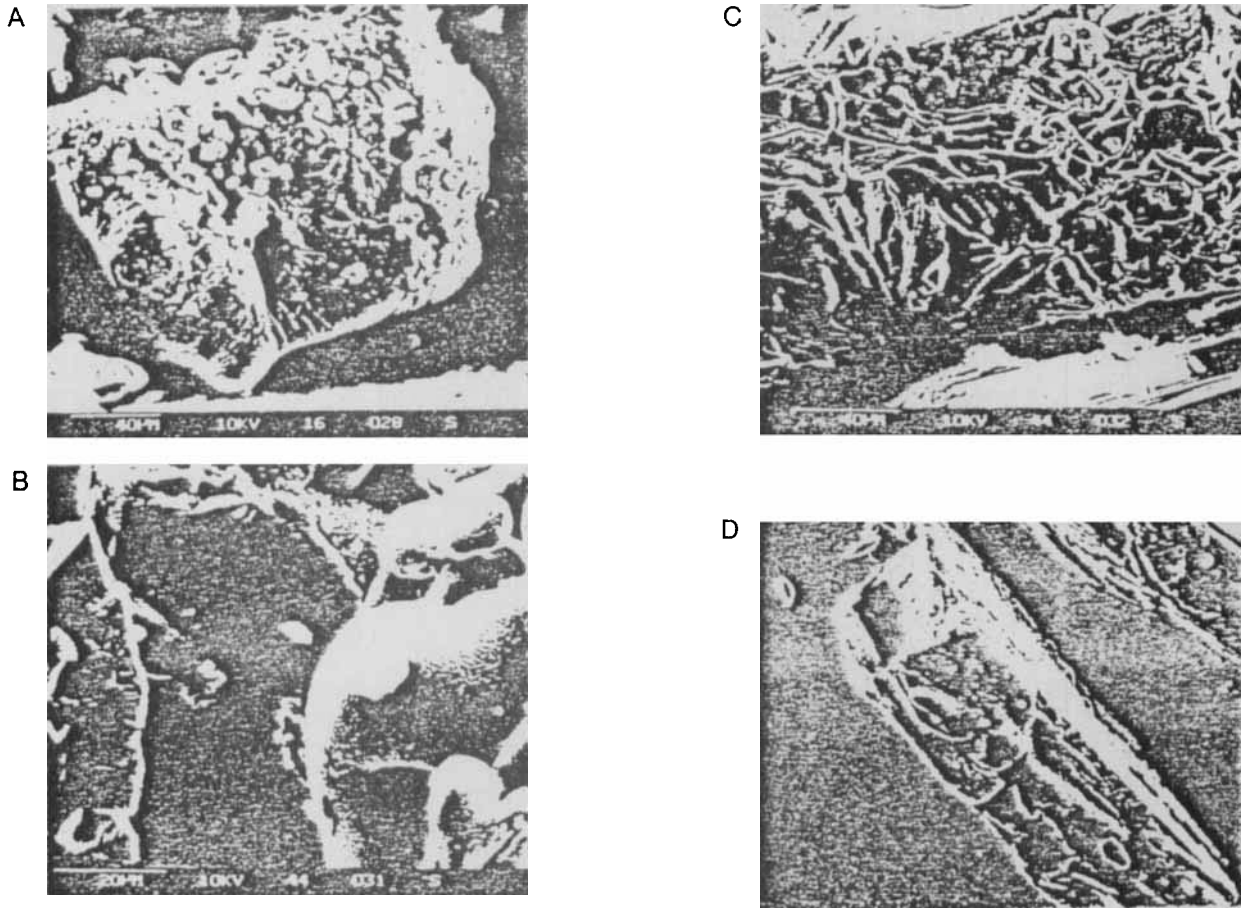

Figure 8—*Scanning electron photomicrographs of urapidil pentahydrate* (A), *trihydrate* (B,C), *and monohydrate* (D).

Table V—Behavior of Urapidil Penta- and Monohydrates under Various Conditions: Differential Scanning Calorimetry Studies

Storage Time, months	Conditions of Storage	Form III, J g^{-1}	Form II, J g^{-1}	Form I, J g^{-1}
Pentahydrate				
0	—	2.68	—[a]	76.41
3	room temp	1.05	4.98	73.86
3	37 °C	22.73	—	81.01
3	37 °C; 80% RH	3.81	—	72.77
1	45 °C	—	—	97.51
3	45 °C	—	—	96.00
Monohydrate				
0	—	—	9.96	86.37
3	room temp	13.90	—	82.31
3	37 °C	0.88	62.43	31.02
3	37 °C; 80% RH	43.42	39.82	5.07
1	45 °C	3.43	19.68	74.99
3	45 °C	1.34	37.76	53.34

[a] Too small to measure.

Monohydrate—The equation relating heat absorbed on dissolution in 95% ethanol at 30 °C was determined to be

$$y = 2.610 \times 10^{2}x + 0.006 \quad (4)$$

with a correlation coefficient of 0.99910 (Figure 7).

The heat absorbed on dissolution, as calculated from the slope of the above equation, was 53.20 kJ mol^{-1} (12.72 kcal mol^{-1}). When calculated for different quantities, the mean heat effect was 53.50 ± 0.81 kJ mol^{-1} (12.74 ± 0.19 kcal mol^{-1}).

A comparison of the heat of solution for the three anhydrous forms, the methanol solvate, as well as the three hydrates of urapidil, can be seen in Table II.

Scanning Electron Microscopy—*Pentahydrate*—No distinctive shape could be identified. Following drying, cracks were visible in the crystal structure, with a few small channels (diameter <8 μm; Figure 8a).

Trihydrate and Monohydrate—Apart from the lack of a characteristic shape, it was also noted that the surfaces of the crystals were flaky. Channels varying in size from 3 to 14 μm

could be seen. The crystal edges were laminated (Figures 8b–d).

Stability of the Hydrates—*Penta- and Monohydrate*—Dehydration occurred for samples stored at 37 and 45 °C (Tables III and IV), while the water content of samples stored at room temperature dropped slightly. Monohydrate samples stored under high relative humidity at 37 °C had an increase to 15.30% of water content (Table IV), while the water content of the pentahydrate increased slightly to 18.62% (Table III). The same DSC thermograms were obtained for both the dehydrated forms due to DSC conditions and storage; namely, mostly Form I (Table V).

Single-Crystal X-ray Analysis—Crystal data for urapidil pentahydrate are listed in Table VI. Final atomic parameters and selected geometrical parameters are given in Tables VII and VIII. The conformation of the urapidil molecule is shown in Figure 9. Its extended nature is the result of the all-trans form of the chain from atoms C(6) to N(11) and the equatorial substitution of the piperazine ring. The latter adopts a chair conformation, with N(11) and N(14) deviating by −0.696(5) and 0.694(5) Å, respectively, from the plane ('plane I') of the four ring C atoms. Interplanar dihedral angles which describe the relative orientations of the ring systems (plane II = uracil, plane III = phenyl) are: I/II 36.3, I/III 42.2, and II/III 6.0° (esd 0.2°).

Relevant torsion angles are listed in Table IX. The conformation observed here differs from that of the urapidil molecule in the 1:1 methanol solvate,[4] where the torsion angles for C(9)—C(10)—N(11)—C(12) [−66.2(4)°], C(15)—N(14)—C(17)—C(18) [169.4(3)°], and C(9)—C(18)—O(18)—C(23) [8.0(5)°] are noted as differing significantly from their counterparts in the pentahydrate. Considerably different drug–solvent hydrogen bonding arrangements occur in the two solvates. Figure 10 is the (010) projection of the crystal structure. The water molecules in each unit cell occupy regions centered around a pair of symmetry-related screw diads. Their y-coordinates span the entire length of the *b* cell dimension, so that continuous, water-filled channels result.

A complex network of hydrogen bonds links the water molecules to one another and to host drug molecules. This arrangement is shown in the stereoscopic view (Figure 11), and relevant distances and angles for the 10 distinct hydrogen bonds are listed in Table X.

Table VI—Crystal Data

Molecular formula	$C_{20}H_{29}N_5O_3 \cdot 5H_2O$	a = 15.421(8) Å
Molecular mass	477.56	b = 10.994(5)
Crystal system	Monoclinic	c = 15.177(8)
Space group	$P2_1/n$	β = 101.72(2)°
Z	4	V = 2519(2) Å^3
D_c, g cm^{-3}	1.259	$F(000)$ = 1032
μ(Mo − Kα), cm^{-1}	0.91	—

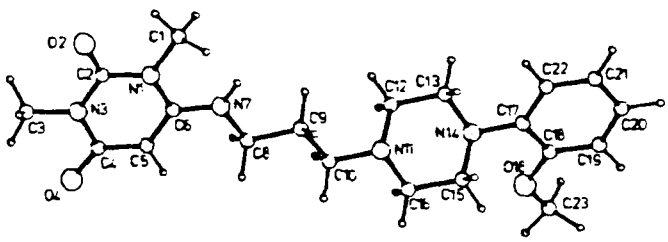

Figure 9—*Conformation of the urapidil molecule in crystals of the pentahydrate.*

Table VII—Fractional Atomic Coordinates for Refined Atoms and Equivalent Isotropic Thermal Parameters[a]

Atom	Fractional Atomic Coordinates[b]			U_{eq}/U_{iso}[c,d]
	x	y	z	
N(1)	5326(3)	3471(4)	9169(3)	32(1)[d]
C(1)	4724(4)	2571(5)	8633(4)	48(2)
C(2)	5766(4)	3103(5)	10023(4)	38(2)
O(2)	5653(3)	2092(3)	10308(3)	49(2)
N(3)	6325(3)	3960(4)	10513(3)	33(2)
C(3)	6811(4)	3591(5)	11421(3)	48(2)
C(4)	6459(4)	5120(5)	10211(4)	37(2)
O(4)	6973(2)	5816(3)	10723(2)	48(2)
C(5)	6009(3)	5430(5)	9334(3)	35(2)
C(6)	5445(3)	4613(5)	8822(4)	34(1)[d]
N(7)	4997(3)	4861(4)	7984(3)	39(2)
C(8)	5110(4)	6028(5)	7553(3)	42(3)
C(9)	4508(4)	6071(5)	6611(3)	41(2)
C(10)	4652(4)	7232(5)	6115(4)	45(3)
N(11)	4060(3)	7286(4)	5221(3)	35(2)
C(12)	4357(4)	6446(5)	4583(3)	42(2)
C(13)	3740(4)	6511(5)	3661(3)	38(2)
N(14)	3747(3)	7750(4)	3292(3)	34(2)
C(15)	3449(4)	8622(5)	3923(3)	44(2)
C(16)	4058(4)	8533(5)	4853(3)	42(2)
C(17)	3238(4)	7861(5)	2387(4)	37(2)
C(18)	3369(4)	8910(5)	1893(4)	38(2)
O(18)	3996(3)	9720(3)	2309(2)	49(2)
C(19)	2882(4)	9070(5)	1019(4)	43(2)
C(20)	2291(4)	8167(6)	631(4)	52(3)
C(21)	2192(4)	7127(6)	1089(4)	57(3)
C(22)	2655(4)	6971(5)	1962(4)	47(3)
C(23)	4257(4)	10664(5)	1774(4)	59(3)
OW(1)	760(3)	6374(5)	8594(3)	75(2)
OW(2)	1878(3)	4664(4)	6210(3)	59(2)
OW(3)	2268(3)	6732(4)	5368(3)	54(2)
OW(4)	1480(3)	4341(5)	7902(3)	66(2)
OW(5)	3599(4)	3583(5)	6830(4)	95(3)
H(1AW)	21(3)	641(6)	845(4)	69[d]
H(1BW)	95(4)	573(5)	825(4)	69[d]
H(2AW)	195(4)	533(4)	600(4)	56[d]
H(2BW)	149(3)	419(4)	586(4)	56[d]
H(3AW)	283(3)	687(5)	528(4)	51[d]
H(3BW)	207(3)	746(4)	551(4)	51[d]
H(4AW)	193(3)	404(5)	827(3)	59[d]
H(4BW)	165(4)	451(5)	736(3)	59[d]
H(5AW)	311(4)	378(6)	666(4)	79[d]
H(5BW)	379(4)	282(5)	660(4)	79[d]
H(7)	458(3)	429(4)	769(3)	53(6)[d]

[a] Estimated standard deviations are given in parentheses. [b] Fractional atomic coordinates are expressed × 10^4, and ×10^3 for H atoms. [c] $U_{eq} = \frac{1}{3}\Sigma_i\Sigma_j U_{ij}\, a_i^* a_i^* a_i a_j$. [d] Isotopic thermal parameters (U_{iso}) are expressed as Å^2 × 10^3.

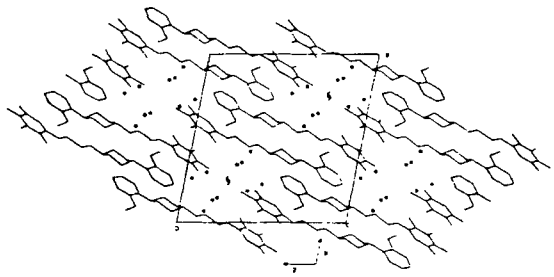

Figure 10—*The (010) projection of the crystal structure of urapidil pentahydrate. The oxygen atoms of the water molecules are represented by filled circles.*

Of the five unique water molecules, only one [associated with atom OW(3)] binds two urapidil molecules directly via a host—H_2O—host hydrogen bond, the remaining bridges

Table VIII—Selected Bond Distances and Bond Angles[a]

Bond Length, Å			
N(1)—C(1)	1.482(7)	C(9)—C(10)	1.521(8)
N(3)—C(3)	1.485(6)	C(10)—N(11)	1.475(7)
N(1)—C(2)	1.395(7)	N(11)—C(12)	1.477(7)
C(2)—N(3)	1.387(7)	N(11)—C(16)	1.480(7)
N(3)—C(4)	1.385(7)	C(13)—N(14)	1.474(7)
C(2)—O(2)	1.218(7)	C(15)—N(14)	1.492(7)
C(4)—O(4)	1.252(6)	C(12)—C(13)	1.526(6)
C(4)—C(5)	1.412(7)	C(15)—C(16)	1.531(6)
C(5)—C(6)	1.376(7)	N(14)—C(17)	1.442(7)
N(1)—C(6)	1.388(7)	C(18)—O(18)	1.371(7)
C(6)—N(7)	1.346(7)	O(18)—C(23)	1.425(7)
N(7)—C(8)	1.467(7)	N(7)—H(7)	0.95(4)
C(8)—C(9)	1.539(6)	—	—

Bond Angle, °	
C(6)—N(1)—C(2)	122.5(5)
N(1)—C(2)—N(3)	115.7(5)
C(2)—N(3)—C(4)	124.5(5)
N(3)—C(4)—C(5)	117.2(5)
C(4)—C(5)—C(6)	120.5(5)
C(5)—C(6)—N(1)	119.6(5)
C(6)—N(7)—C(8)	120.9(5)
C(6)—N(7)—H(7)	119(3)
C(8)—N(7)—H(7)	120(3)
N(7)—C(8)—C(9)	109.7(5)
C(8)—C(9)—C(10)	111.4(5)
C(9)—C(10)—N(11)	111.3(5)
C(10)—N(11)—C(12)	111.2(5)
C(10)—N(11)—C(16)	109.8(4)
C(12)—N(11)—C(16)	108.0(4)
C(15)—N(14)—C(17)	112.2(4)
C(13)—N(14)—C(17)	113.3(4)
C(13)—N(14)—C(15)	108.8(4)
N(11)—C(12)—C(13)	110.7(5)
C(12)—C(13)—N(14)	109.9(4)
N(14)—C(15)—C(16)	109.8(5)
C(15)—C(16)—N(11)	111.1(5)
C(18)—O(18)—C(23)	117.7(5)

[a] Estimated standard deviation in parentheses.

Table IX—Selected Torsion Angles

	Angle, °[a]
N(1)—C(6)—N(7)—C(8)	−177.7(5)
C(6)—N(7)—C(8)—C(9)	−179.0(5)
N(7)—C(8)—C(9)—C(10)	−176.1(5)
C(8)—C(9)—C(10)—N(11)	−178.7(5)
C(9)—C(10)—N(11)—C(12)	−74.2(6)
C(9)—C(10)—N(11)—C(16)	166.3(5)
N(11)—C(12)—C(13)—N(14)	61.3(6)
C(12)—C(13)—N(14)—C(15)	−59.4(6)
C(13)—N(14)—C(15)—C(16)	58.3(6)
N(14)—C(15)—C(16)—N(11)	−58.9(6)
C(15)—C(16)—N(11)—C(12)	58.6(6)
C(16)—N(11)—C(12)—C(13)	−59.5(6)
C(13)—N(14)—C(17)—C(22)	12.1(8)
C(15)—N(14)—C(17)—C(18)	71.2(7)
C(19)—C(18)—O(18)—C(23)	−10.1(8)

[a] Estimated standard deviation in parentheses.

Table X—Hydrogen Bonding Geometry

D—H...A[a]	D...A, Å	H...A, Å	D—H...A, °
N(7)—H(7)...OW(5)	2.856(7)	1.94(4)	161(4)
OW(1)—H(1BW)...OW(4)	2.794(8)	1.86(6)	163(5)
OW(2)—H(2AW)...OW(3)	2.734(7)	1.93(5)	169(5)
OW(3)—H(3AW)...N(11)	2.882(7)	1.97(5)	174(5)
OW(4)—H(4BW)...OW(2)	2.782(7)	1.86(5)	171(5)
OW(5)—H(5AW)...OW(2)	2.886(7)	2.12(6)	169(6)
OW(2)—H(2BW)...O(2^{i})[b]	2.849(6)	1.98(5)	168(5)
OW(4)—H(4AW)...O(4^{ii})	2.838(5)	2.04(5)	153(5)
OW(3)—H(3BW)...O(4^{iii})	2.804(6)	1.93(5)	162(5)
OW(5)—H(5BW)...OW(1^{iv})	2.747(8)	1.79(6)	169(6)

[a] D = donor, A = acceptor. [b] Symmetry code: (i) $-\frac{1}{2} + x, \frac{1}{2} - y, -\frac{1}{2} + z$; (ii) $1 - x, 1 - y, 2 - z$; (iii) $-\frac{1}{2} + x, 1\frac{1}{2} - y, -\frac{1}{2} + z$; (iv) $\frac{1}{2} - x, -\frac{1}{2} + y, 1\frac{1}{2} - z$.

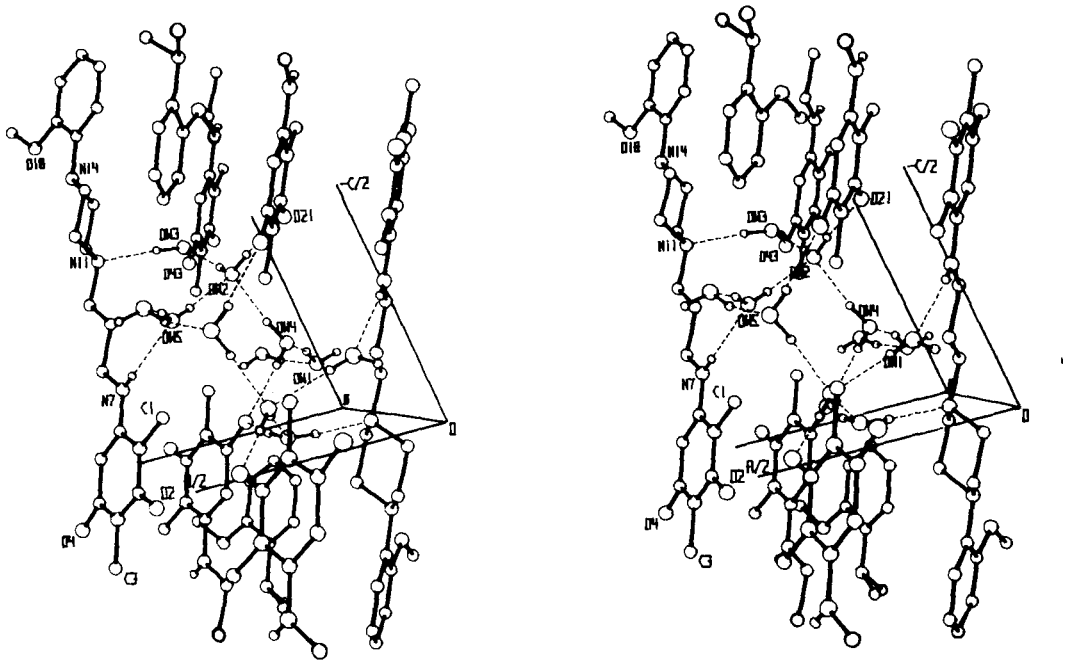

Figure 11—*Stereoview showing hydrogen bonds (dashed lines) arranged around one of the twofold screw axes. (The latter is tilted about 15° away from the view direction.) For clarity, H atoms of urapidil are omitted, except for H(7), which participates in hydrogen bonding.*

between host molecules being effected by chains of hydrogen-bonded water molecules. The extent to which individual water molecules participate in hydrogen bonding varies widely and ranges over engagement in two [for atom OW(1)], three [for each of OW(3), OW(4), and OW(5)], and four [for OW(2)] hydrogen bonds. The structural model is therefore consistent with the TGA data, which indicate a stepwise loss of water on desolvation of the pentahydrate. Since the water molecules are the principal source of cohesion in the crystal (there being no hydrogen bonds linking urapidil molecules directly), it is not surprising that desolvation results in a polymorph (Form I) that is characterized by a different powder pattern.

References and Notes

1. Schoetensack, W.; Bischler, P.; Dittman, E. Ch.; Steinijans, V. *Arzneim.-Forsch.* **1977**, *27*, 1908–1919.
2. Barnakay, A.; Göb, E.; Richter, J. A. *Arzneim.-Forsch.* **1981**, *31*, 849–852.
3. Botha, S. A.; Guillory, J. K.; Lötter, A. P. *J. Pharm. Biomed. Anal.* **1986**, *4*, 573–587.
4. Botha, S. A.; Caira, M. R.; Guillory, J. K.; Lötter, A. P. *J. Pharm. Biomed. Anal.*, in press.
5. Sheldrick, G. M. *Program for crystal structure determination*, SHELX76; University of Cambridge, England, 1976.
6. De Wet, J. F. *J. Appl. Crystallogr.* **1980**, *13*, 625–629.
7. Nardelli, M. *Comput. Chem.* **1983**, *7*, 95–98.
8. Singh, P.; Desai, S. J.; Flanagan, D. R.; Simonelli, A. P.; Higuchi, W. K. *J. Pharm. Sci.* **1968**, *57*, 959–965.
9. Stagner, W. C.; Guillory, J. K. *J. Pharm. Sci.* **1979**, *68*, 1005–1009.

Acknowledgments

Urapidil was generously provided by Dr. M. H. Durr, Byk Gulden Pharmaceuticals, Randburg, South Africa. The authors thank Dr. V. E. Hamilton-Attwell, Department of Zoology, and Dr. A. M. Viljoen, Department of Chemistry, University of Potchefstroom for C. H. E., in whose laboratories the SEM photomicrographs and IR spectra were recorded. One of us (MRC) thanks the CSIR (Pretoria) for financial assistance and the NPRL for providing the intensity data-collection service. This study was initiated at the College of Pharmacy, University of Iowa, and completed at the Faculty of Pharmacy, University of Potchefstroom for C. H. E., South Africa. The work was supported in part by a grant from Marion Laboratories. This study was abstracted in part from a dissertation submitted by S. A. Botha to the Faculty of Pharmacy, University of Potchefstroom for C. H. E., in partial fulfillment of the Doctor of Scientiae degree requirement.